Stochastic modeling of transient surface scalar and momentum fluxes in turbulent boundary layers

Marten Klein[1]* · Heiko Schmidt[1] · David O. Lignell[2]

[1]Numerical Fluid and Gas Dynamics, Brandenburg University of Technology, Cottbus, Germany – *Contact: marten.klein@b-tu.de
[2]Chemical Engineering, Brigham Young University, Provo, UT, USA

Introduction

Turbulence is ubiquitous in **atmospheric boundary layers** and manifests itself by **transient transport processes** on a **range of scales** (e.g. [1, 2]). This range easily reaches down to less than a meter, which is smaller than the typical height of the first grid cell layer adjacent to the surface in **numerical models** for weather and climate prediction on the global and regional scale (e.g. [3, 4]). In these models, the **bulk-surface coupling** plays an important role for the evolution of the atmospheric boundary layer (e.g. [5, 6]) but it is not feasible to fully resolve it in applications (e.g. [7]). Hence, the overall fidelity of numerical weather and climate predictions crucially depends on the modeling of small (subfilter) scale transport processes in the vicinity of the surface. A **standing challenge** in this regard is the **economical but accurate modeling** of transient, intermittent, and non-Fickian transport processes (e.g. [8, 9]) and counter-gradient fluxes (e.g. [10]) that arise from the interplay of forcing, diffusion, rotation, and stratification effects. We address the issues mentioned above by utilizing a **stochastic one-dimensional turbulence (ODT)** [11] model.

Main objectives

- Investigation of **surface-flux fluctuations** by resolving dominating **transient boundary layer processes**.
- **Modeling** using a numerical tool applicable throughout the **relevant parameter space**.
- Capturing **wall-normal (vertical) transport processes** on **all relevant scales** of the flow by utilizing the **one-dimensional turbulence** model [11].

ODT model formulation

The **ODT model** aims to **resolve all relevant scales** of a turbulent flow along a notional line-of-sight ('ODT line'). Flow variables are resolved along this line on a dynamically adaptive grid [12]. Instantaneous flow profiles are evolved by **deterministic diffusion** along the ODT domain, and a **stochastic process** that models the effects of turbulent advection, pressure fluctuations, and buoyancy forces that are aligned with the ODT domain (wall-normal coordinate) [11, 13, 14].

- The **ODT governing equations** for rotating stratified boundary layers are

$$\frac{\partial u_i}{\partial t} + \mathcal{E}_i(u,v,w,\rho;\alpha) = \nu\frac{\partial^2 u_i}{\partial z^2} - f\,\epsilon_{i3k}\,(u_k - G\,\delta_{k1}) + S_i\,, \qquad \frac{\partial T}{\partial t} + \mathcal{E}_T(u,v,w,\rho) = \kappa\frac{\partial^2 T}{\partial z^2} + S_T\,,$$

where z denotes the wall-normal coordinate, t the time, $(u_i) = (u,v,w)^\mathrm{T}$ with $i \in \{1,2,3\}$ the Cartesian components of the velocity vector, T the (potential) temperature and $\rho(T) = \rho_0[1-(T-T_0)/T_0]$ the mass density in the Oberbeck–Boussinesq approximation (subscript 0 indicates reference values), ν and κ the fluid's kinematic viscosity and thermal diffusivity, respectively, $f = 2\Omega$ the inertial frequency of horizontal Coriolis forces, Ω the system's angular velocity, G the geostrophically balanced bulk flow velocity, S_i and S_T the specific momentum and thermal sources, respectively, and ε_{ijk} the Levi–Civita tensor.

- **Stochastic terms** $\mathcal{E}_i$ and $\mathcal{E}_T$ represent the effects of discrete **eddy events**. For each stochastically sampled eddy event, the turnover of a notional turbulent eddy (**Fig. 1(a)**) is modeled by the instantaneous application of the **triplet map** [11] (**Fig. 1(b)**).
- The turbulent **eddy rate** $\tau^{-1}(\ell, z_0; t)$ of a size-ℓ eddy event at location z_0 at time t depends on the **total available eddy specific energy** for the momentary flow state. The eddy rate reads [11, 14]

$$\tau^{-1} = C\sqrt{2\,\ell^{-2}\,(E_\mathrm{kin} - E_\mathrm{pot} - Z\,E_\mathrm{vp})}\,,$$

where E_kin and E_pot denote the eddy specific kinetic and potential energy, respectively, and E_vp is a viscous penalty energy to suppress eddy events below a viscous length scale [11].

- The **ODT model parameters** $C = 6$ (eddy-rate parameter), $Z = 1$ (viscous-suppression parameter), and $\alpha = 2/3$ (pressure-scrambling efficiency) have been fixed after calibration with reference direct numerical simulation (DNS) [16, 15] for velocity statistics in neutrally-stratified Ekman flow.

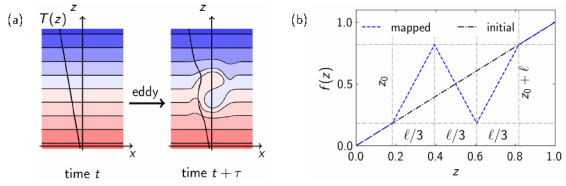

Figure 1: (a) Schematic of an eddy turnover. (b) Triplet map for an eddy event that covers the interval $0.18 \leqslant z \leqslant 0.82$.

Laminarization in stably-stratified Ekman flow

Stable stratification may entirely suppress turbulence which is an effect that underlies the **laminarization** in the nocturnal atmospheric surface layer (e.g. [8, 6, 17]). Under dry conditions, strong near-wall stratification may arise from radiative cooling. Here we consider a prescribed **sudden surface cooling event** [15] that gives rise to transient evolution. The flow is governed by boundary conditions such that heat and momentum sources vanish ($S_T \equiv 0$, $S_i \equiv 0$). The flow is governed by the Prandtl (Pr), Reynolds (Re), Froude (Fr) and bulk Richardson (Ri) numbers

$$Pr = \frac{\nu}{\kappa} \simeq 1\,, \qquad Re = \frac{G\,D}{\nu}\,, \qquad Fr = \frac{G^2}{g\,D\,(T_\mathrm{bulk} - T_0)/T_0}\,, \qquad Ri = \frac{g\,D_\star(T_\mathrm{bulk} - T_0)/T_0}{G^2}\,.$$

- **Fig. 2(a)** shows a sketch of the **stable boundary-layer configuration** investigated.
- **Fig. 2(b)** shows the **vertical structure** for the **mean horizontal velocity** of the laminar and turbulent neutrally-stratified ($T = T_0$) initial condition. U is the geostrophic and V the ageostrophic mean velocity component, respectively. The **Ekman layer thickness** $D = \sqrt{2\nu/f}$ of the laminar solution (e.g. [18] is taken as reference length scale. $D_\star > D$ is the **turbulent boundary layer thickness**.

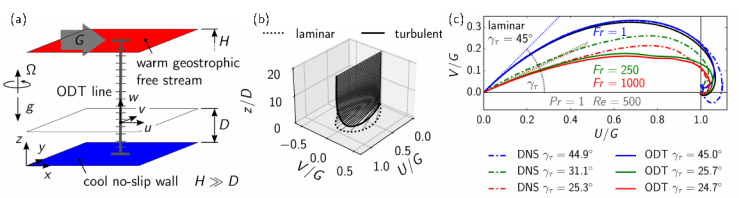

Figure 2: (a) Sketch of the stratified Ekman flow configuration. (b) Ekman spiral of the ensemble-averaged horizontal velocity for laminar and turbulent flow. (c) Hodographs of the ensemble-averged horizontal velocity X inertial periods after the cooling event for $Re = 500$, $Pr = 1$, and various Fr. The wind-turning angles γ_τ are also given. The near-surface flow has laminarized for $Fr = 1$ in ODT but already for $Fr = 100$ in the corresponding reference DNS [15].

- **Fig. 2(c)** shows **hodographs** ('Ekman spirals') of the ensemble-averaged velocities $U(z,t_0)$ and $V(z,t_0)$ for various Fr at fixed times t_0. DNS [15] are given after one ($t_0 = 2\pi/f$) and ODT after two ($t_0 = 4\pi/f$) inertial periods $2\pi/f$. The 'kink' in the ODT results is a modeling artifact that occurs at a finite distance from the wall. The near-surface flow laminarizes for low $Fr \lesssim 100$. The **wind-turning angles** $\gamma_\tau = \arctan\left[(\mathrm{d}V/\mathrm{d}z)_0/(\mathrm{d}U/\mathrm{d}z)_0\right]$ are measured at the surface and exhibit reasonable agreement.

Horizontal velocity fluctuations in neutrally-stratified Ekman flow

The **neutrally-stratifed Ekman boundary layer** is a canonical case for the well-mixed atmospheric boundary layer (e.g. [8]). High resolution requirements arise from **small-scale near-wall processes** that exhibit length scales as small as the Ekman layer thickness, that is, $D \sim O(10\,\mathrm{cm})$ in Earth's mid-latitude atmosphere. Current work focuses on improving circulation models and parameterization schemes (e.g. [2]).

- **Fig. 3(a)** shows **horizontal velocity fluctuations** by a scatter plot of $N = 500$ instantaneous velocity hodographs of an ODT simulation for low Re encompassing tens of inertial periods. The variability is effectively bounded by the laminar Ekman spiral and the fixed geostrophic wind direction.
- **Fig. 3(b)** shows the **probability density function (p.d.f.)** of the **wind-turning angle** γ_τ obtained with ODT for various Re in comparison to global observations as compiled in [19]. ODT is generally consistent with the IGRA and SPARC sounding ensembles but encompasses here a smaller range of values. The ERA-Interim reanalysis underestimates the ageostrophic flow due to unresolved near-surface processes.

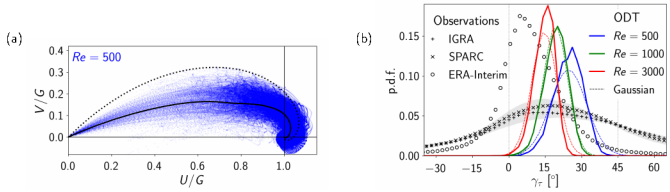

Figure 3: (a) Scatter plot of $N = 500$ instantaneous hodographs of the horizontal velocity for neutrally-stratified Ekman flow from an ODT simulation over several inertial periods. (b) Probability density function (p.d.f.) of the wind-turning angle γ_τ showing preliminary ODT results together with observations (for details, see [19] and references therein).

Surface-flux fluctuations in weakly-heated channel flow

In the **weakly-heated channel**, the perturbation temperature T is treated as **passive scalar** such that there are no potential energy contributions to the ODT eddy rate. The flow is driven by a prescribed **mean pressure gradient** $S_i = -\delta_{i1}\,\rho_0^{-1}\,(\mathrm{d}P/\mathrm{d}x)$ and the scalar is injected by a prescribed **mean heat flux** q_w. By compensating for the mean heating, a source term S_T is obtained for the perturbation temperature [20, 21]. The **ODT model parameter values** for channel flow are $C = 6$, $Z = 300$, $\alpha = 1/6$ [21].

- **Fig. 4(a)** shows a sketch of the **weakly-heated channel configuration**
- **Fig. 4(b)** and **Fig. 4(c)** show the **joint probability density functions** of **surface scalar** ($q'_\mathbf{w}$) **and momentum** ($\tau'_\mathbf{w}$) **flux fluctuations** for ODT and reference DNS [20], respectively. Here, $Pr = 0.71$ (air) and $Re_\tau = u_\tau\delta/\nu = 1000$, where $u_\tau = \sqrt{\tau_\mathrm{w}/\rho_0}$. ODT satisfactorily captures the state-space and the dissimilarity between the scalar and momentum transfer.

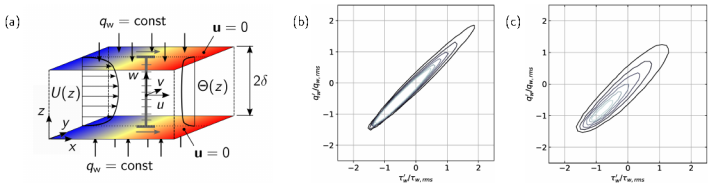

Figure 4: (a) Sketch of the non-rotating weakly-heated channel flow configuration. (b) ODT and (c) DNS [20] prediction of the joint probability density function of surface scalar and momentum flux fluctuations for $Pr = 0.71$ and $Re_\tau = 1000$.

Conclusions

- **Stably-stratified Ekman flow.** – ODT captures **transient effects** due to stratification and rotation in the atmospheric surface layer. The model predicts **near-surface laminarization** for very stable flow conditions.
- **Neutrally-stratified Ekman flow.** – The **p.d.f. of the wind-turning angle** predicted by ODT is consistent with observations for the well-mixed atmospheric boundary layer. The ageostrophic mass transport in the surface layer is more accurately represented than in state-of-the-art reanalysis.
- **Weakly-heated channel flow.** – ODT provides **detailed fluctuation statistics** of scalar *and* momentum surface fluxes for *arbitrary* Re and Pr consistent with DNS.

References

[1] J. R. Garratt, *Earth-Sci. Rev.* **37**, 89 (1994).
[2] L. Mahrt, *Annu. Rev. Fluid Mech.* **46**, 23 (2014).
[3] T. N. Krishnamurti, *Annu. Rev. Fluid Mech.* **27**, 195 (1995).
[4] T. T. Warner, *Numerical Weather and Climate Prediction* (Cambridge University Press, 2010).
[5] A. Z. Owinoh, *et al.*, *Boundary-Layer Meteorol.* **116**, 331 (2005).
[6] B. J. H. van de Wiel, *et al.*, *J. Atmos. Sci.* **69**, 3116 (2012).
[7] M. A. Jiménez, J. Cuxart, *Boundary-Layer Meteorol.* **115**, 241 (2005).
[8] A. A. M. Holtslag, F. T. M. Nieuwstadt, *Boundary-Layer Meteorol.* **36**, 201–209 (1986).
[9] C. Ansorge, J. P. Mellado, *J. Fluid Mech.* **805**, 611 (2016).
[10] J. W. Deardorff, *J. Atmos. Sci.* **23**, 503 (1966).
[11] A. R. Kerstein, *J. Fluid Mech.* **392**, 277 (1999).
[12] D. O. Lignell, A. R. Kerstein, G. Sun, E. I. Monson, *Theor. Comp. Fluid Dyn.* **27**, 273 (2013).
[13] A. R. Kerstein, W. T. Ashurst, S. Wunsch, V. Nilsen, *J. Fluid Mech.* **447**, 85 (2001).
[14] A. R. Kerstein, S. Wunsch, *Boundary-Layer Meteorol.* **118**, 325 (2006).
[15] C. Ansorge, J. P. Mellado, *Boundary-Layer Meteorol.* **153**, 89 (2014).
[16] P. R. Spalart, G. N. Coleman, R. Johnstone, *Phys. Fluids* **20**, 101507 (2008).
[17] L. Mahrt, *Boundary-Layer Meteorol.* **90**, 375 (1999).
[18] J. Pedlosky, *Geophysical Fluid Dynamics* (Springer-Verlag, 1979).
[19] J. Lindvall, G. Svensson, *Q. J. R. Meteorol. Soc.* **145**, 3074 (2019).
[20] H. Abe, H. Kawamura, Y. Matsuo, *Int. J. Heat Fluid Flow* **25**, 404 (2004).
[21] M. Klein, H. Schmidt, D. O. Lignell, Stochastic modeling of surface scalar-flux fluctuations in turbulent channel flow using one-dimensional turbulence (2021). Submitted.